AKADÉMIAI KIADÓ

Preventive effect of *Lactobacillus plantarum* YS1 isolated from naturally fermented yoghurt on carrageenan-induced thrombosis in mice

M.-W. Wang[1†], F. She[2†], J. Song[1], Y.-Q. Liu[1], X.-Y. Long[1], X. Zhao[1*] and H.-Q. Hong[3*]

[1] Collaborative Innovation Center for Child Nutrition and Health Development, Chongqing University of Education, Chongqing, China

[2] Department of Emergency, the Fourth Medical Center of the Chinese PLA General Hospital, Beijing, China

[3] Department of Emergency, First Affiliated Hospital of Gannan Medical University, Ganzhou, Jiangxi, China

ORIGINAL RESEARCH PAPER

© 2023 The Author(s)

ABSTRACT

This work used a carrageenan-based thrombosis model to determine the preventative effects of *Lactobacillus plantarum* YS1 (LPYS1) on thrombus. In thrombotic mice, LPYS1 improved the activated partial thromboplastin time (APTT), while decreasing the thrombin time (TT), prothrombin time (PT), and fibrinogen (FIB) content. In thrombotic mouse serum, LPYS1 decreased the levels of malondialdehyde (MDA), tumour necrosis factor-alpha (TNF-α), interleukin-6 (IL-6), nuclear factor kappa-B (NF-κB), and interleukin-1 beta (IL-1β), while also increasing the activities of superoxide dismutase (SOD) and catalase (CAT). Moreover, LPYS1 upregulated the mRNA expression levels of copper/zinc-SOD (Cu/Zn-SOD), manganese-SOD (Mn-SOD), and CAT in the colon tissues of thrombotic mice, while downregulating those of NF-κB p65, IL-6, TNF-α, and interferon-gamma (IFN-γ) mRNA. In tail vein vascular tissues, LPYS1 suppressed the mRNA expression levels of NF-κB p65, intercellular cell adhesion molecule-1 (ICAM-1),

* Corresponding authors. E-mail: zhaoxin@cque.edu.cn, a01230@gmu.edu.cn

† Mengwei Wang and Fei She contributed equally to this work.

AKJournals

vascular cell adhesion molecule-1 (VCAM-1), and E-selectin. The abundances of both beneficial and pathogenic bacteria were altered by LPYS1. These findings show that LPYS1 has the capacity to protect mice from thrombosis, while also revealing some of the underlying mechanisms of this effect.

1. INTRODUCTION

Following behind hypertension and heart disease, thrombosis is also becoming a common condition in the middle-aged and elderly population (Rodríguez et al., 2006). To address this issue, increasingly more studies are being conducted on thrombolytic medications and anti-thrombotic dietary additives (Xu et al., 2021). Intraperitoneal carrageenan administration has been found to cause intestinal irritation in test animals. Numerous inflammatory mediators and free radicals are released during inflammation, thereby harming vascular endothelial cells and causing thrombosis. Because there is only one caudal artery in the mouse tail, its embolisation greatly impedes the ability of collateral circulation to resume, thereby leading to progressive ischemia and necrosis of the mouse tail tissues (Arslan et al., 2010). In this study, a mouse model of thrombosis was established using carrageenan-induced inflammation to induce tail vein thrombosis.

Yak yogurt is a food product produced from fermented milk that is typically consumed in ethnic minority areas of China's plateau. Both the flavour and microbial community of yak yogurt are also exceptionally rich due to the plateau's unique temperature, altitude, and processing methods. Laboratory investigations in mice have demonstrated that lactic acid bacteria isolated from naturally fermented yak milk can reduce alcoholic liver injury, inhibit d-galactose-induced oxidative senescence, and reduce alcoholic stomach injury via a mechanism involving increased antioxidant activity (Long et al., 2022).

The measurement of four of the blood coagulation components APTT, TT, PT, and FIB are essential in the clinical diagnosis of blood diseases involving faulty coagulation (Jing, 2020). When a thrombus develops, a large proportion of available coagulation factors are used up, thereby lengthening the PT, whereas a shortage of coagulation factors shortens the APTT. Bodily blood flow is continuously maintained, while FIB is continuously converted by the action of thrombin into fibrin, which is the major component of a thrombus. The body speeds up the process of fibrinolysis and produces more fibrin breakdown products when the blood's fibrin content is too high, which prolongs the TT (Wang et al., 2016).

The crucial role that oxidative stress plays in thrombosis is illustrated by the ability of free radical scavengers to completely prevent thrombosis induced by iron ions. SOD is crucial for preserving the balance between oxidation and anti-oxidation in the body, because it has the ability to catalyse the disproportionation of superoxide anion radicals to form oxygen and hydrogen peroxide. The two important SOD types produced by mammals are Cu/Zn-SOD and Mn-SOD (Wolin et al., 2005). The enzymatic activity of CAT also contributes to antioxidant defence, as it is an enzyme scavenger that can promote the breakdown of H_2O_2 into molecular

oxygen and water (Ledesma et al., 2012). Peroxidation occurs when free radicals interact with the lipids in living organisms. Proteins, nucleic acids, and other organic macromolecules cross-link and polymerise as a result of MDA, which is the ultimate consequence of oxidation. Due to MDA's cytotoxic properties, its quantity can both directly and indirectly reflect the extent of lipid peroxidation in the body (Chen et al., 1995).

Inflammation can result in the formation of thrombi, while in turn, thrombi can increase inflammation over time. This positive feedback loop is referred to as "thrombotic inflammation". After inflammation has initiated, TLR may stimulate monocytes, macrophages, lymphocytes, and endothelial cells to increase the production of TNF-α, IL-6, and other inflammatory mediators (Franks et al., 2013). As the initiator of the inflammatory cell cascade, TNF-α controls the subsequent NF-κB and MAPK signalling pathways through its receptor. This causes the activation of numerous cells, including macrophages and lymphocytes, and stimulates the release of IL-6, IL-8, TNF-α, and other inflammatory molecules from macrophages, which exacerbate vascular endothelial damage and deep vein thrombosis (Sochorová et al., 2007). TNF-α and IL-1β cytokines induce the synthesis of vasoconstrictor chemicals, cause vasoconstriction, promote the formation of thrombi, and lower both the transcription and expression of thrombomodulin (TM) in endothelial cells to diminish its anticoagulant activity (Chen et al., 2018).

Because ICAM-1 predominantly promotes the adhesion response between cells and between cells and the matrix, it is a crucial component in both the initiation and further development of inflammation (Kevil et al., 2004). VCAM-1 can negatively affect platelet adhesion and aggregation, as well as trigger inflammatory reactions at thrombus sites (ten Hacken et al., 1998). E-selectin can mediate the local attachment of both leukocytes and vascular endothelial cells in the presence of blood flow, damage endothelial cells via inflammation, increase endothelial cell permeability, and speed up leukocyte exudation (Roth Flach et al., 2013). Endothelial cells can be activated by the NF-κB pathway to initiate an inflammatory response, which subsequently increases the expression of adhesion molecules and cytokines, such as ICAM-1, VCAM-1, and E-selectin. This further activates NF-κB to amplify the inflammatory response, activate platelet aggregation and coagulation, and ultimately create a hypercoagulable state (Xia et al., 2001).

The drug heparin is often used clinically to treat patients with thrombophilia, so heparin was used as the positive drug control in this study. Our team identified a strain of lactic acid bacteria (LPYS1) derived from naturally fermented yak yogurt, which was used in this study. We observed the effect of LPYS1 on thrombosis in mice by regulating their gut microbiota to control their oxidative stress and inflammation levels. This mouse model was used to investigate new uses for the probiotic to prevent thrombosis, assist in the elimination of thrombosis, and reduce the occurrence of various thrombosis-related diseases.

2. MATERIALS AND METHODS

2.1. The experimental bacterial strain

LPYS1 was derived and identified from naturally fermented yak yogurt obtained from Yushu City (Qinghai Province, China) by our team. The strain was assigned the strain collection number M2016747 and placed in the China Center for Type Culture Collection (Wuhan, China).

2.2. Animal treatments

The 50 ICR mice (6-week-old, male, Chongqing Medical University, Chongqing, China) were divided into 5 groups containing 10 mice each: normal, model, heparin (drug positive control), low-concentration LPYS1 (LPYS1-L), and high-concentration LPYS1 (LPYS1-H). Every day, mice in the normal group were administered 0.01 mL of physiological saline solution per g BW intraperitoneally. For 10 days, mice in the other groups received 0.01 mL of 0.2% carrageenan solution per g BW in the intraperitoneal cavity. Simultaneously, mice in model group treated only with carrageenan solution, mice in the heparin group received 20 mg kg^{-1} of heparin daily, whereas mice in the LPYS1-L and LPYS1-H groups received oral administration of 10^8 and 10^9 CFU kg^{-1} LPYS1 daily, respectively. Heparin and LPYS1 were administered by gavage for 10 days. After 10 days, the length of the blackened region in the tail vein (indicating thrombus) in each group of mice was measured (Han et al., 2021). The use of experimental animals was ethically implemented in all activities, including the breeding of experimental mice and other experimental processes (approval number: 202107002B).

2.3. Blood coagulation determination

Before the mice were euthanised, blood was drawn and placed in a centrifuge tube containing sodium citrate. Using a semi-automated hemagglutination system, the plasma was collected, and the four blood coagulation components APTT, TT, PT, and FIB (Wuxi Yuncui Biotechnology Co., Ltd, Wuxi, China) were measured. The semi-automatic coagulation instrument was turned on and preheated to 37 °C, and then the reagents for various detection indicators that need to be preheated were placed in the reagent preheating position for preheating. After the magnetic beads were added to the testing cup and the sample was added, the corresponding results were obtained by starting the testing.

2.4. Identifying oxidation and inflammatory related indicators

Whole blood samples were centrifuged at 4,000 r.p.m. for 10 min at 4 °C to obtain the serum. To assess the serum oxidation indicators, detection kits of SOD, CAT, MDA, TNF-α, IL-6, NF-κB, and IL-1β were used (Shanghai Enzyme Link Biotechnology Co., Ltd, Shanghai, China). After adding various indicators of reagents to serum samples, the OD value was measured using an enzyme-linked immunosorbent assay (ELISA), and the corresponding detection indicator value was calculated based on the formula and standard curve in the kit manual (Hu et al., 2022).

2.5. Quantitative PCR to determine mRNA expression in the mouse tail vein and colon tissues

To extract and homogenise the 50–100 mg of tail vein and colon tissue, 1 mL of Trizol reagent (Invitrogen, New York, NY, USA) was used. A 1.5 mL centrifuge tube was filled with homogenised tail vein and colon tissue. 200 μL of chloroform was then put in. The tube was centrifuged for 15 min at 4 °C and 14,000 r.p.m. after being at 4 °C for 5 min. A fresh 1.5 mL centrifuge tube was filled with the RNA-containing supernatant. Isopropanol was added in an equal amount and blended. The tube was then centrifuged at 14,000 r.p.m. for 20 min at 4 °C after being at 4 °C for 15 min. The supernatant was removed after centrifugation, and the RNA precipitate was collected. After washing the RNA precipitate with a 75% ethanol solution, it was centrifuged

at 14,000 r.p.m. and 4 °C for 15 min. The top aqueous phase was discarded following centrifugation. The centrifuge tube cap was opened, and it was left open for 3–5 min. The RNA was then dissolved using 20 µL of RNase-Free water (Thermo Fisher Scientific, Waltham, MA, USA) and diluted to a concentration of 1 µg µL^{-1}. Following the directions, Thermo Fisher Scientific's Revert Aid First Strand cDNA synthesis kit was used to mix with 1 µL RNA solution to form a final reaction solution of 20 µL, which was then reverse transcribed into cDNA. The cDNA was subsequently amplified using PCR. The amplification set-up included 10 µL of Mastermix from Thermo Fisher Scientific, 1 µL of each of the forward and reverse sequence primers (10 µmol L^{-1}) from the same manufacturer (Thermo Fisher Scientific, Table 1), 1 µL of cDNA, and 7 µL of sterile ultrapure water. The following amplification conditions were used (Onestep Plus, Thermo Fisher Scientific): denaturation at 95 °C for 3 min, annealing at 60 °C for 20 s, extension at 72 °C for 1 min, the above reactions were cycled 30 times, then extension again at 72 °C for 10 min. The relative mRNA expression levels of each target gene were then computed using the formula below, using GAPDH as the housekeeping gene:

$$2^{-\Delta\Delta Ct} = 2^{-[(Ct\ treated\ sample\ target\ gene\ -\ Ct\ treated\ sample\ housekeeping\ gene)\ -\ (Ct\ control\ sample\ target\ gene\ -\ Ct\ control\ sample\ housekeeping\ gene)]}$$ (Hu et al., 2022).

2.6. Statistical investigation

Each experimental test was repeated three times in parallel on a technical level. Standard deviations were obtained after determining the average value of the measurement data. The experimental data were reported as the means and standard deviations. A one-way analysis of variance ($P < 0.05$) was used to identify significant differences between groups.

3. RESULTS AND DISCUSSION

3.1. APTT, TT, FIB, and PT in mice

The TT (18.7 ± 1.6 min) and PT (3.7 ± 0.4 min) of the normal group mice were shorter than those of the other groups, but the APTT (201.8 ± 13.3 min) was longer and the FIB content (52.1 ± 6.1 g L^{-1}) was the lowest ($P < 0.05$, Fig. 1). The TT (79.8 ± 5.5 min) and

Table 1. The used primer sequences of this study

| Gene	Forward sequence	Reverse sequence
Cu/Zn-SOD	5′-AACCAGTTGTGTTGTGAGGAC-3′	5′-CCACCATGTTTCTTAGAGTGAGG-3′
Mn-SOD	5′-CAGACCTGCCTTACGACTATGG-3′	5′-CTCGGTGGCGTTGAGATTGTT-3′
CAT	5′-GGAGGCGGGAACCCAATAG-3′	5′-GTGTGCCATCTCGTCAGTGAA-3′
NF-κB p65	5′-GAGGCACGAGGCTCCTTTTCT-3′	5′-GTAGCTGCATGGAGACTCGAACA-3′
ICAM-1	5′-TCCGCTACCATCACCGTGTAT-3′	5′-TAGCCAGCACCGTGAATGTG-3′
VCAM-1	5′-TTGGGAGCCTCAACGGTACT-3′	5′-GCAATCGTTTTGTATTCAGGGGA-3′
E-selectin	5′-ATAACGAGACGCCATCATGC-3′	5′-TGTCCACTGCCCTTGTGC-3′
IL-6	5′-ATGAAGTTCCTCTCTGCAA-3′	5′-AGTGGTATCCTCTGTGAAG-3′
TNF-α	5′-ATGGGGGGCTTCCAGAA-3	5′-CCTTTGGGGACCGATCA-3′
IFN-γ	5′-GCTTTGCAGCTCTTCCTCAT-3′	5′-GTCACCATCCTTTTGCCAGT-3′
GAPDH	5′-TGACCTCAACTACATGGTCTACA-3′	5′-CTTCCCATTCTCGGCCTTG-3′
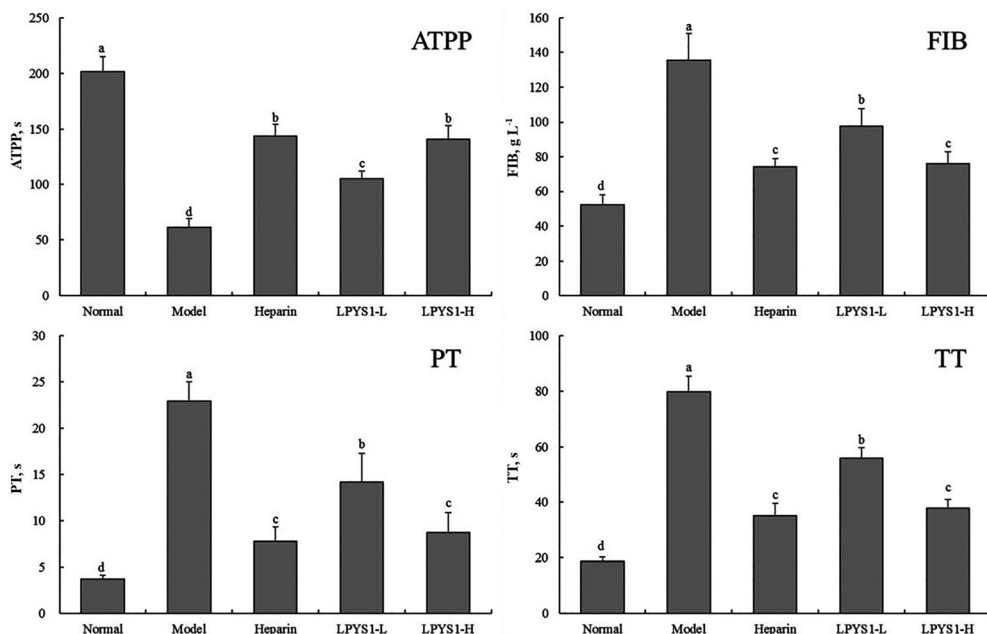
Fig. 1. The mice with thrombosis' thrombin time (TT), fibrinogen (FIB), activated partial thromboplastin time (APTT), and prothrombin time (PT). [a–d] The mean values in the several bars with different letters are noticeably different, according to Duncan's multiple range test, the same lowercase letters indicate no significant difference ($P > 0.05$), and different lowercase letters indicate significant difference ($P < 0.05$) between the corresponding two groups (Same on Figs 2–5)

PT (22.9 ± 2.1 min) of the model group were shorter than those of the other groups, while the APTT (61.3 ± 7.8 min) was the longest and the FIB content (135.6 ± 15.4 g L^{-1}) was the highest ($P < 0.05$). Although the TT (37.8 ± 3.1 min) and PT (8.7 ± 2.2 min) of the LPYS1-H group were shorter than those of the LPYS1-L group (55.9 ± 3.9 min and 14.2 ± 3.1 min), and the FIB content (75.9 ± 7.1 g L^{-1}) was also lower than that of the LPYS1-L group (97.8 ± 9.8 g L^{-1}), the APTT of the LPYS1-H group was significantly longer (140.9 ± 12.1 min, $P < 0.05$) than LPYS1-L group (105.2 ± 6.9 min). There were no significant differences ($P > 0.05$) in APTT, TT, FIB, or PT between the LPYS1-H group and the heparin group.

APTT, TT, PT, and FIB are important coagulation and thrombus detection indicators in clinical practice, therefore they were also used for validation in this study (Jing, 2020). Heparin and LPYS1 were engaged in controlling the four blood coagulation markers measured in this study, they may be able to prevent thrombosis. LPYS1 was found to increase the levels of the blood coagulation markers in a concentration-dependent manner.

3.2. SOD, CAT, and MDA in mice

The normal group of mice had the significantly ($P < 0.05$) lowest content of MDA (15.56 ± 3.12 mmol mL^{-1}) and the highest SOD (378.20 ± 22.36 U mL^{-1}) and CAT (91.08 ± 6.75 U mL^{-1}) enzyme activities of all groups, according to the findings of the blood tests (Fig. 2). The SOD
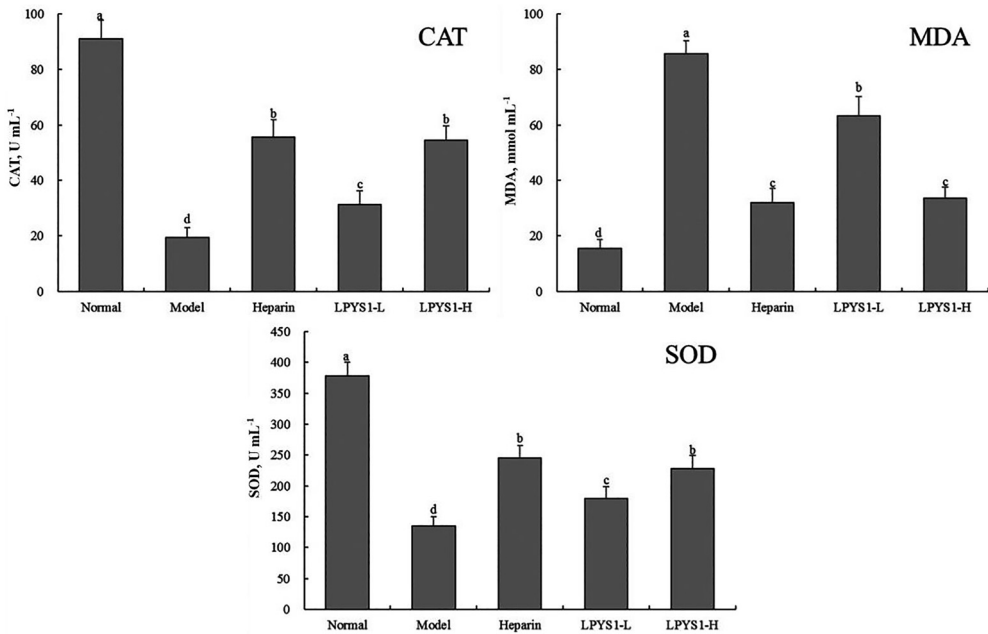
Fig. 2. The serum levels of SOD, CAT, and MDA in thrombotic mice

and CAT enzyme activity levels were marginally higher in the heparin (245.67 ± 20.14 U mL^{-1}, 55.71 ± 6.21 U mL^{-1}) and LPYS1-H (228.35 ± 21.09 U mL^{-1}, 54.61 ± 5.08 U mL^{-1}) groups when compared to the normal group, while they were marginally lower in the LPYS1-L (179.58 ± 18.98 U mL^{-1}, 31.25 ± 4.98 U mL^{-1}) group when compared to the normal group. The SOD and CAT enzyme activity levels were significantly ($P < 0.05$) the lowest in the model group mice (134.54 ± 15.53 U mL^{-1} and 19.37 ± 3.65 U mL^{-1}, respectively). The MDA level was significantly ($P < 0.05$) the highest in the model group (85.61 ± 4.68 mmol mL^{-1}), and the LPYS1-H group (33.56 ± 3.98 mmol mL^{-1}) had lower values than LPYS1-L group (63.21 ± 7.12 mmol mL^{-1}).

Free radical build-up plays a critical function in both initiating and exacerbating thrombosis. When exposed to ROS, platelets are significantly more vulnerable to the three platelet aggregation substances thrombin, collagen, and arachidonic acid, in addition to being directly activated (Yamashita et al., 2015). These results suggest that a close relationship exists between thrombosis and oxidative stress. Because the impact of LPYS1 at the highest experimental dosage matched that of antithrombotic medications in this study, LPYS1 appears to have good prospects in assisting certain oxidation-related markers to return to near-normal levels.

3.3. TNF-α, IL-6, NF-κB, and IL-1β in mice

The levels of TNF-α, IL-6, NF-κB, and IL-1β increased in the corresponding group order: the normal, heparin, LPYS1-H, LPYS1-L, and model groups (Fig. 3). The heparin (132.06 ± 19.87 pg mL^{-1}, 51.23 ± 5.65 pg mL^{-1}, 352.06 ± 21.03 pg mL^{-1}, 105.35 ± 20.22 pg mL^{-1}) and LPYS1-H (140.36 ± 21.36 pg mL^{-1}, 54.66 ± 6.01 pg mL^{-1}, 361.77 ± 3.24 pg mL^{-1},
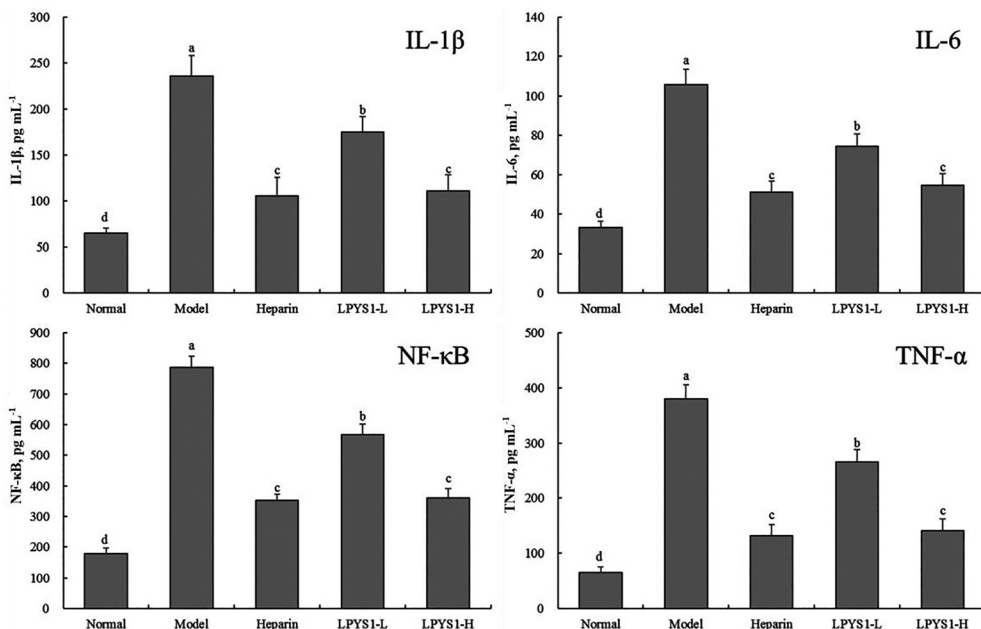
Fig. 3. The TNF-α, IL-6, NF-κB, and IL-1β concentrations in the serum of mice with thrombosis

111.25 ± 17.63 pg mL^{-1}) groups had significantly ($P < 0.05$) lower levels of TNF-α, IL-6, NF-κB, and IL-1β than the LPYS1-L (265.31 ± 22.97 pg mL^{-1}, 74.29 ± 6.42 pg mL^{-1}, 567.89 ± 33.35 pg mL^{-1}, 175.25 ± 16.86 pg mL^{-1}) group. However, there was no statistically significant difference between the LPYS1-H group and heparin group.

Therefore, by modulating TNF-α, IL-6, NF-κB, and IL-1β, the inflammatory response may be controlled so that thrombus formation is prevented. Limiting thrombus development is another strategy. In this study, heparin's interference with the inflammatory cytokines listed above led to an inhibitory impact on thrombosis. A comparable role was also played by high-concentration LPYS1, which had a positive intervening impact on both inflammatory cytokines and thrombosis.

3.4. mRNA expression of Cu/Zn-SOD, Mn-SOD, CAT, NF-κB p65, IL-6, TNF-α, and IFN-γ in mouse colon tissues

The mRNA expression levels of Cu/Zn-SOD, Mn-SOD, and CAT in the colon tissues of mice were the significantly ($P < 0.05$) highest in the normal group, while being the lowest in the model group, according to the qPCR results (Fig. 4). The mRNA expression levels of Cu/Zn-SOD, Mn-SOD, and CAT in mouse colon tissues were comparable between the LPYS1-H and heparin groups, which were significantly ($P < 0.05$) higher than those in the LPYS1-L group.

The model group of mice had significantly ($P < 0.05$) higher mRNA expression levels of NF-κB p65, IL-6, TNF-α, and IFN-γ in their colon tissues than the other groups, while the normal group of mice had markedly ($P < 0.05$) lower levels in all groups. In the colon tissues
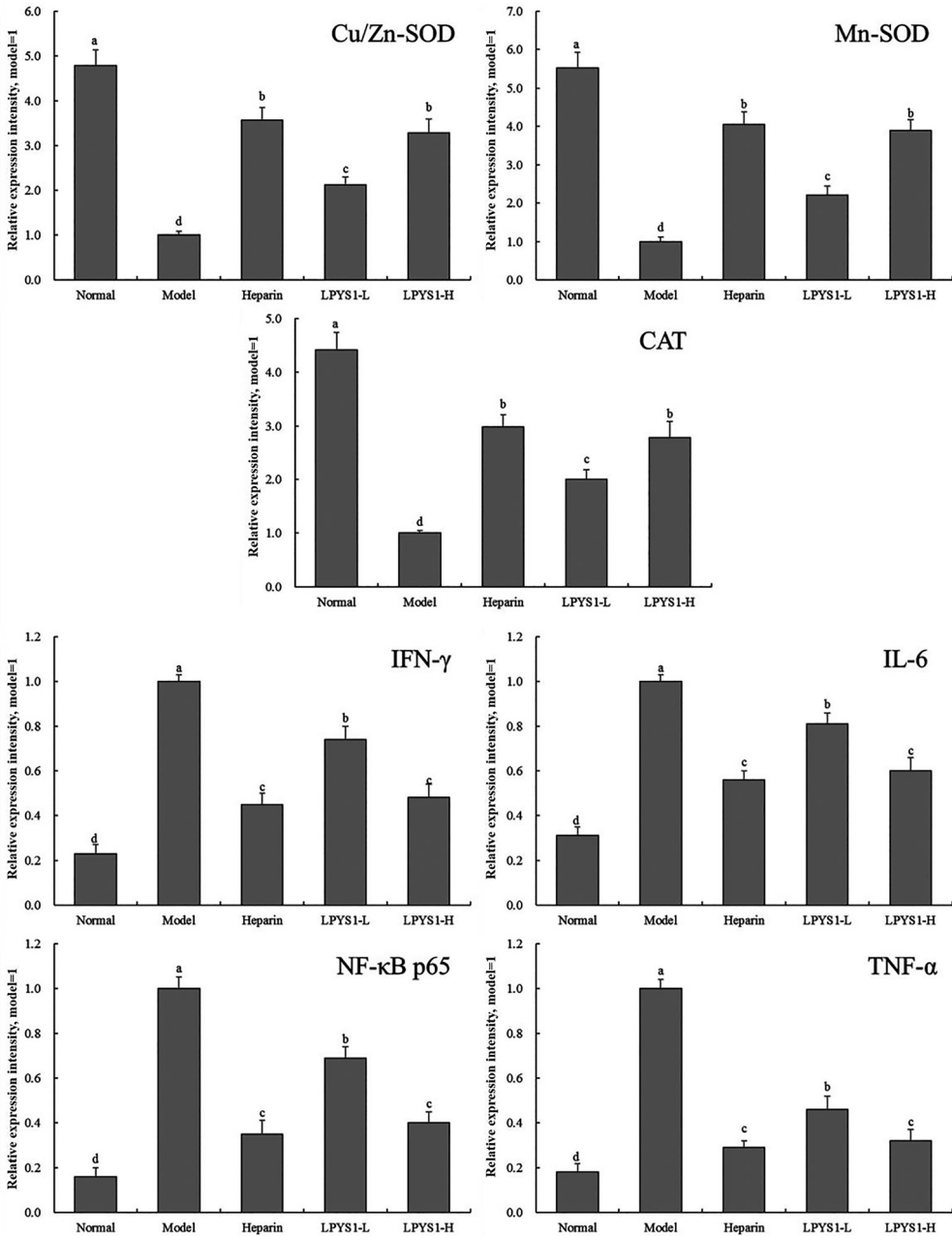
Fig. 4. The expression of mRNA for Cu/Zn-SOD, Mn-SOD, CAT, NF-κB p65, IL-6, TNF-α, and IFN-γ in colon tissues from thrombotic mice

of thrombotic mice, NF-κB p65, IL-6, TNF-α, and IFN-γ mRNA production was inhibited by both LPYS1 and heparin. Heparin and LPYS1-H both exhibited comparable outcomes and were notably more efficient in decreasing the expression of the above mRNAs than LPYS1-L.

The mRNA expression experiment results are similar to the previous results of serum oxidative stress and inflammatory cytokine detection, further verifying the effectiveness and mechanism of LPYS1 in regulating oxidative stress and inflammatory response to intervene in thrombosis.

3.5. mRNA expression of NF-κB p65, ICAM-1, VCAM-1, and E-selectin in mouse tail vein tissues

In the tail vein, the model group of mice had the highest levels of NF-B p65, ICAM-1, VCAM-1, and E-selectin mRNA expression ($P < 0.05$, Fig. 5). In the thrombotic tail vein of mice, the heparin, LPYS1-L, and LPYS1-H treatments were all able to considerably lower the mRNA expression levels of NF-B p65, ICAM-1, VCAM-1, and E-selectin. The ability of LPYS1-H and heparin to reduce these expressions was significantly ($P < 0.05$) stronger than that of LPYS1-L.

In the case of increased NF-κB activity, the expression of pro-inflammatory molecules increases. It was demonstrated that the interrelated expression levels of ICAM-1, VCAM-1, and E-selectin in the NF-κB-centric pathway differed significantly from those at the baseline state.
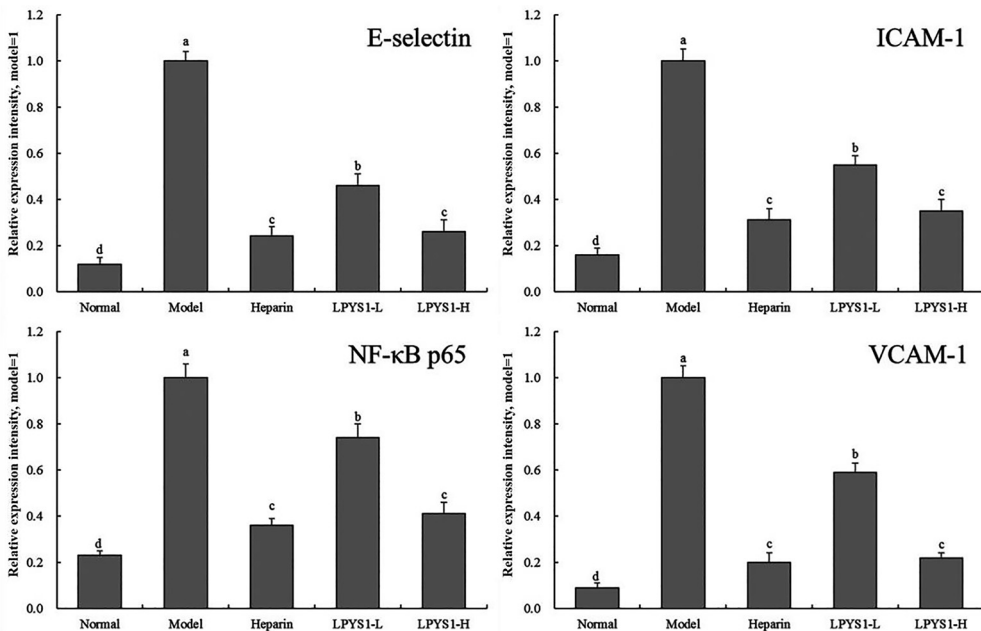

Fig. 5. The expression of mRNA for ICAM-1, VCAM-1, E-selectin, and NF-κB p65 in tail vein tissues from thrombotic mice

4. CONCLUSIONS

In this study, we investigated the potential of the recently discovered bacteria LPYS1 to prevent mouse thrombosis. This research shows that LPYS1 could regulate mouse intestinal function and protect against thrombosis by reducing oxidative stress and inflammation. The mechanisms by which probiotics exert their effects in the human body are complex and diverse. LPYS1, for instance, has the ability to colonise the intestinal tract in large numbers. It is believed that LPYS1 may exert its antioxidant effects by improving gut microbiota, modulating the immune system, and clearing harmful substances in the intestines. Optimisation of the gut microbiota environment plays a role in promoting digestion and absorption, enhancing physical fitness, and resisting inflammation (Kouhidhi et al., 2021). What makes it even more complex is that the active substances produced by LPYS1's metabolites have beneficial effects on the body. Among them, there may be complex substances that can regulate blood clotting and have an effect when they enter the bloodstream. Therefore, on one hand, further clinical research and human trials are needed to confirm the efficacy of LPYS1. On the other hand, a more in-depth study is required to understand the specific mechanisms of action of LPYS1 itself and its metabolites, especially in identifying key metabolites that play a crucial role. However, preliminary research in this study has confirmed that LPYS1 has a positive effect on thrombosis intervention in animal organisms, suggesting its potential as a good probiotic and its value for development and utilisation.

ACKNOWLEDGEMENTS

REFERENCES

Arslan, R., Bor, Z., Bektas, N., Meriçli, A.H., and Ozturk, Y. (2010). Antithrombotic effects of ethanol extract of *Crataegus orientalis* in the carrageenan-induced mice tail thrombosis model. *Thrombosis Research*, 127(3): 210–213.

Chen, L.Y., Nichols, W.W., Hendricks, J., and Mehta, J.L. (1995). Myocardial neutrophil infiltration, lipid peroxidation, and antioxidant activity after coronary artery thrombosis and thrombolysis. *American Heart Journal*, 129(2): 211–218.

Chen, X., Han, R., Hao, P., Wang, L., Liu, M., Jin, M., Kong, D., and Li, X. (2018). Nepetin inhibits IL-1β induced inflammation via NF-κB and MAPKs signaling pathways in ARPE-19 cells. *Biomedicine & Pharmacotherapy*, 101: 87–93.

Franks, Z., Campbell, R.A., Vieira de Abreu, A., Holloway, J.T., Marvin, J.E., Kraemer, B.F., Zimmerman, G.A., Weyrich, A.S., and Rondina, M.T. (2013). Methicillin-resistant *Staphylococcus aureus*-induced thrombo-

inflammatory response is reduced with timely antibiotic administration. *Thrombosis and Haemostasis*, 109(4): 684–695.

Han,. Z.Y., Shen, S.Y., Zhang, J.X., Zhou, Y., Zhao, X., Liu, M.J., and Xu, X.L. (2021). Preliminary establishment of chronic thrombus model in mice. *Acta Laboratorium Animalis Scientia Sinica*, 29(1): 78–84.

Hu, T., Chen, R., Qian,Y., Ye, K., Long, X., Park, K.Y., and Zhao, X. (2022). Antioxidant effect of *Lactobacillus fermentum* HFY02-fermented soy milk on D-galactose-induced aging mouse model. *Food Science and Human Wellness*, 11(5): 1362–1372.

Jing, F. (2020). Comparative study of four items of hemagglutination in different degrees of diffuse intravascular coagulation. *China Modern Medicine*, 27(8): 162–165. (In Chinese with English abstract).

Kevil, C.G., Pruitt, H., Kavanagh, T.J., Wilkerson, J., Farin, F., Moellering, D., Darley-Usmar, V.M., Bullard, D.C., and Patel, R.P. (2004). Regulation of endothelial glutathione by ICAM-1: implications for inflammation. *FASEB Journal*, 18(11): 1321–1323.

Kouidhi, S., Souai, N., Zidi, O., Mosbah, A., Lakhal, A., Ben Othmane, T., Belloumi, D., Ben Ayed, F., Asimakis, E., Stathopoulou, P., Cherif, A., and Tsiamis, G. (2021). High Throughput analysis reveals changes in gut microbiota and specific fecal metabolomic signature in hematopoietic stem cell transplant patients. *Microorganisms*, 9(9): 1845.

Ledesma, J.C., Font, L., and Aragon, C.M. (2012). The H_2O_2 scavenger ebselen decreases ethanol-induced locomotor stimulation in mice. *Drug and Alcohol Dependence*, 124(1–2): 42–49.

Long, X.Y., Wang, P., Zhou, Y.J., Wang, Q., Ren, L.X., Li, Q., Zhao, X. (2022). Preventive effect of *Lactobacillus plantarum* HFY15 on carbon tetrachloride (CCl_4)-induced acute liver injury in mice. *Journal of Food Science*, 87(6): 2626–2639.

Rodríguez, T., Malvezzi, M., Chatenoud, L., Bosetti, C., Levi, F., Negri, E., and La Vecchia, C. (2006). Trends in mortality from coronary heart and cerebrovascular diseases in the Americas: 1970–2000. *Heart*, 92(4): 453–460.

Roth Flach, R.J., Matevossian, A., Akie, T.E., Negrin, K.A., Paul, M.T., and Czech, M.P. (2013). β3-Adrenergic receptor stimulation induces E-selectin-mediated adipose tissue inflammation. *The Journal of Biological Chemistry*, 288(4): 2882–2892.

Sochorová, K., Horváth, R., Rozková, D., Litzman, J., Bartunková, J., Sedivá, A., and Spísek, R. (2007). Impaired Toll-like receptor 8-mediated IL-6 and TNF-alpha production in antigen-presenting cells from patients with X-linked agammaglobulinemia. *Blood*, 109(6): 2553–2556.

ten Hacken, N.H., Postma, D.S., Bosma, F., Drok, G., Rutgers, B., Kraan, J., and Timens, W. (1998). Vascular adhesion molecules in nocturnal asthma: a possible role for VCAM-1 in ongoing airway wall inflammation. *Clinical and Experimental Allergy*, 28(12): 1518–1525.

Wang, X., Kong, D., and Li, W. (2016). Effects of aqueous extracts from *Cyclocarya paliurus* leaves on blood lipids, hemagglutination, and lipid peroxidation in rats with diabetic nephropathy. *Modern Food Science & Technology*, 32(6): 1–6. (In Chinese with English abstract).

Wolin, M.S., Ahmad, M., and Gupte, S.A. (2005). Oxidant and redox signaling in vascular oxygen sensing mechanisms: basic concepts, current controversies, and potential importance of cytosolic NADPH. *American Journal of Physiology*, 289(2): 159–173.

Xia, Y.F., Liu, L.P., Zhong, C.P., and Geng, J.G. (2001). NF-kappaB activation for constitutive expression of VCAM-1 and ICAM-1 on B lymphocytes and plasma cells. *Biochemical and Biophysical Research Communications*, 289(4): 851–856.

Xu, M., Chen, R., Liu, L., Liu, X., Hou, J., Liao, J., Zhang, P., Huang, J., Lu, L., Chen, L., Fan, M., Chen, X., Zhu, X., Liu, B., and Hu, P. (2021). Systemic immune-inflammation index and incident cardiovascular

diseases among middle-aged and elderly Chinese adults: the Dongfeng-Tongji cohort study. *Atherosclerosis*, 323: 20–29.

Yamashita, T., Sato, T., Sakamoto, K., Ishii, H., and Yamamoto, J. (2015). The free-radical scavenger edaravone accelerates thrombolysis with alteplase in an experimental thrombosis model. *Thrombosis Research*, 135(6): 1209–1213.